


RESEARCH ARTICLE

Expanding the genetic and clinical spectrum of the NONO-associated X-linked intellectual disability syndrome

Colleen M. Carlston^{1,2}  | Steven B. Bleyl³ | Ashley Andrews⁴ | Lindsay Meyers³ | Sara Brown² | Pinar Bayrak-Toydemir^{1,2} | James F. Bale⁵ | Lorenzo D. Botto⁴

¹Department of Pathology, University of Utah, Salt Lake City, Utah

²ARUP Institute for Clinical and Experimental Pathology, Salt Lake City, Utah

³Division of Pediatric Cardiology, University of Utah, Salt Lake City, Utah

⁴Division of Medical Genetics, University of Utah, Salt Lake City, Utah

⁵Department of Pediatric Neurology, University of Utah, Salt Lake City, Utah

Correspondence

Colleen Carlston, School of Medicine, University of California, 513 Parnassus Ave, S245, San Francisco, CA 94143.
Email: colleen.carlston@ucsf.edu

The *NONO* gene encodes a nuclear protein involved in RNA metabolism. Hemizygous loss-of-function *NONO* variants have been associated with syndromic intellectual disability and with left ventricular noncompaction (LVNC). A two-year-old boy presented to the University of Utah's Penelope Undiagnosed Disease Program with developmental delay, nonfamilial features, relative macrocephaly, and dilated cardiomyopathy with LVNC and Ebstein anomaly. Brain MRI showed a thick corpus callosum, mild Chiari I malformation, and a flattened pituitary. Exome sequencing identified a novel intronic deletion (c.154+5_154+6delGT) in the *NONO* gene. Splicing studies demonstrated intron 4 read-through and the use of an alternative donor causing the frameshift p.Asn52Serfs*6. Family segregation analysis showed that the variant occurred de novo in the boy's unaffected mother. MRI and endocrine findings suggest that hypopituitarism may contribute to growth failure, abnormal thyroid hormone levels, cryptorchidism, or delayed puberty in patients with *NONO*-associated disease. Also, including this case LVNC has been observed in five out of eight patients, and this report also confirms an association between loss of *NONO* and Ebstein anomaly. In some cases, unrelated individuals share the same pathogenic *NONO* variants but do not all have clinically significant LVNC, suggesting that additional modifiers may contribute to cardiac phenotypes.

KEYWORDS

Ebstein anomaly, left ventricular noncompaction, *NONO*, splicing variant, syndromic intellectual disability

1 | INTRODUCTION

The nonoctamer-containing, POU-domain DNA-binding protein (*NONO*) is a highly conserved, member of the *Drosophila* behavior/human splicing (DBHS) protein family thought to be involved in various aspects of RNA metabolism (Shav-Tal and Zipori, 2002). Mice lacking *NONO* have small cerebellums, spatial memory impairment, and changes at inhibitory synapses (Mircsof et al., 2015). Immunohistochemistry indicates that *NONO* is broadly expressed in mouse tissues, including in neurons and granule cells of the cortex and hippocampus (Mircsof et al., 2015) as well as in the heart (Scott et al., 2017). Hemizygous loss-of-function variants in the Xq13.1-located *NONO* gene in patients were initially associated with an intellectual disability syndrome (MIM: 300967), with findings including macrocephaly, nonfamilial features, and thickened corpus callosum (Mircsof et al., 2015). Subsequently, four additional patients were

described with these features and with left ventricular noncompaction (LVNC) cardiomyopathy (Reinstein et al., 2016; Scott et al., 2017). To date, five pathogenic *NONO* alterations have been reported, two of which were observed twice in unrelated patients. Notably, identical *NONO* variants were variably associated with LVNC. Here we report a patient with shared as well as additional features that confirm and expand the physical, functional, and cardiovascular phenotypes associated with *NONO* loss.

2 | CLINICAL REPORT

This two-year-old boy at the time of testing was the first-born child of healthy, nonconsanguineous parents and has a healthy younger sister. Prenatal-onset growth failure with preservation of head circumference

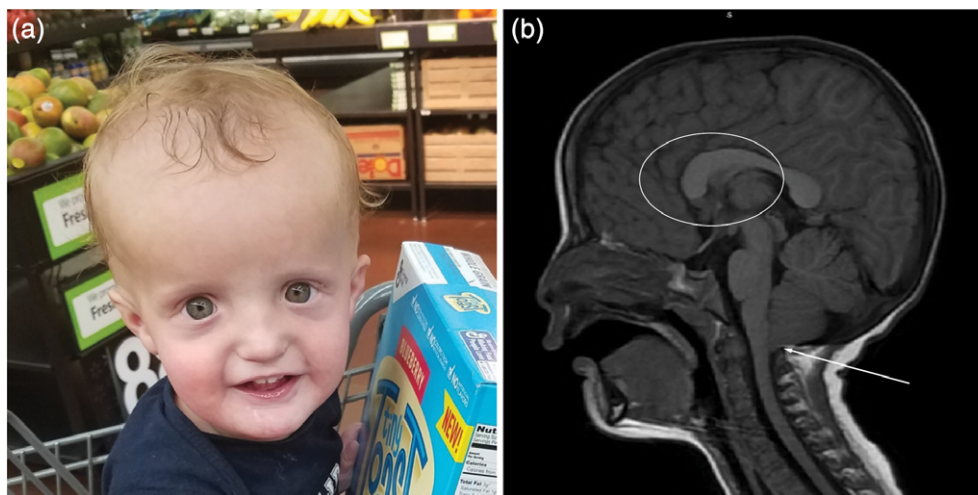


FIGURE 1 Patient phenotype. (a) a photograph of the boy at age two demonstrates relative macrocephaly, a triangular face, widely spaced eyes, downslanted palpebral fissures, malar flattening, and a thin vermilion of the upper lip. (b) MRI at 20 months of age shows abnormalities that include a thickened corpus callosum, especially at the genu and splenium (white circle), a mild Chiari I malformation (white arrow), and a shallow Sella turcica with a flattened pituitary gland [Color figure can be viewed at wileyonlinelibrary.com]

was noted at full term birth (birth weight 2.5 kg). He developed failure to thrive, silent tracheal aspiration, regurgitation, and feeding intolerance, and was provided nasogastric feedings to optimize nutrition. By 2 years of age he was tracking below the first percentile for both height and weight (8.7 kg), though his head size was relatively large (OFC 50 cm). Laboratory evaluation repeatedly indicated growth hormone deficiency and intermittently low thyroid hormone. Growth hormone replacement therapy was initiated; by 32 months of age he had gained some weight (10.2 kg) but was still below the first percentile for height and weight, with OFC at the 96th percentile (52 cm).

Global developmental delay was diagnosed based on delayed speech, motor delays, and sensory processing issues. The boy spoke his first words at 15 months of age but periodically gained and lost words. He began to cruise at approximately 18 months of age and could pull to stand. While using a walker he walked with a mildly wide-based gait. Cranial nerve examination showed mild pseudobulbar palsy and muscle stretch reflexes were trace.

Cardiology evaluation with echocardiography at 2 months of age showed (a) dilated left ventricle with myocardial noncompaction (dense apical trabeculations) and decreased systolic and diastolic left ventricular function; (b) Ebsteinoid tricuspid valve tethering with mild regurgitation; (c) patent foramen ovale with left to right shunting. Subsequent evaluations by physical exam, echocardiogram, and electrocardiogram did not indicate progressive cardiovascular disease despite being diagnosed with Ross classification Class I and ACC/AHA Stage C heart failure at age 4 months.

The patient's presentation and history also included surgically-corrected exotropia, severe mixed central/obstructive sleep apnea, bilateral inguinal testes at birth that descended without intervention by age three (retractile), and a single episode of fungal esophagitis. On exam, he was noted to have a triangular face, widely spaced eyes, downslanted palpebral fissures, malar flattening, and a thin vermilion of the upper lip (Figure 1a). An MRI performed in infancy was motion-compromised but found no overt structural abnormalities. A repeat MRI performed at

20 months of age detected a thick genu of the corpus callosum, a mild Chiari I malformation, and a flattened pituitary gland (Figure 1b).

Previous nondiagnostic testing included a SNP microarray, Noonan syndrome gene panel, dilated cardiomyopathy panel, Russell-Silver syndrome methylation testing, urine organic acids, plasma amino acids, free and total carnitine, creatine kinase, lactate, and ammonia. Mild elevations in C5DC/C10OH were interpreted as likely secondary to dietary supplements. Due to the complexity of the presentation and the extensive prior assessments that had not identified a diagnosis, the family was evaluated by the Penelope Undiagnosed and Rare Disease Program. Through this program at the University of Utah a multidisciplinary team undertook a comprehensive evaluation of the patient, who then underwent exome sequencing.

3 | METHODS

3.1 | Exome sequencing and analysis

Capture enrichment was performed on DNA extracted from peripheral blood using Illumina SureSelect XT kit reagents (Agilent Technologies, Santa Clara, CA). Samples were sequenced on a HiSeq2500 platform (Illumina, San Diego, CA) using paired-end 100 bp reads. All rare (<1% population frequency) coding variants and variants within 10 bases of an intron-exon junction were evaluated. Predicted molecular consequences of variants were assessed using Alamut Visual v2.10 (Interactive Software). Sanger sequencing was performed using Big Dye[®] Terminator v3.1 and an ABI 3730 DNA Analyzer (Life Technologies, Carlsbad, CA).

3.2 | cDNA amplification, sequencing, and qPCR

RNA was extracted using a Promega Maxwell[®] 16 instrument from peripheral blood within 48 hr of draw, and reverse transcribed into cDNA with random hexamers. Two sets of primers in exons flanking intron 4 of the NONO mRNA were used to amplify the region in

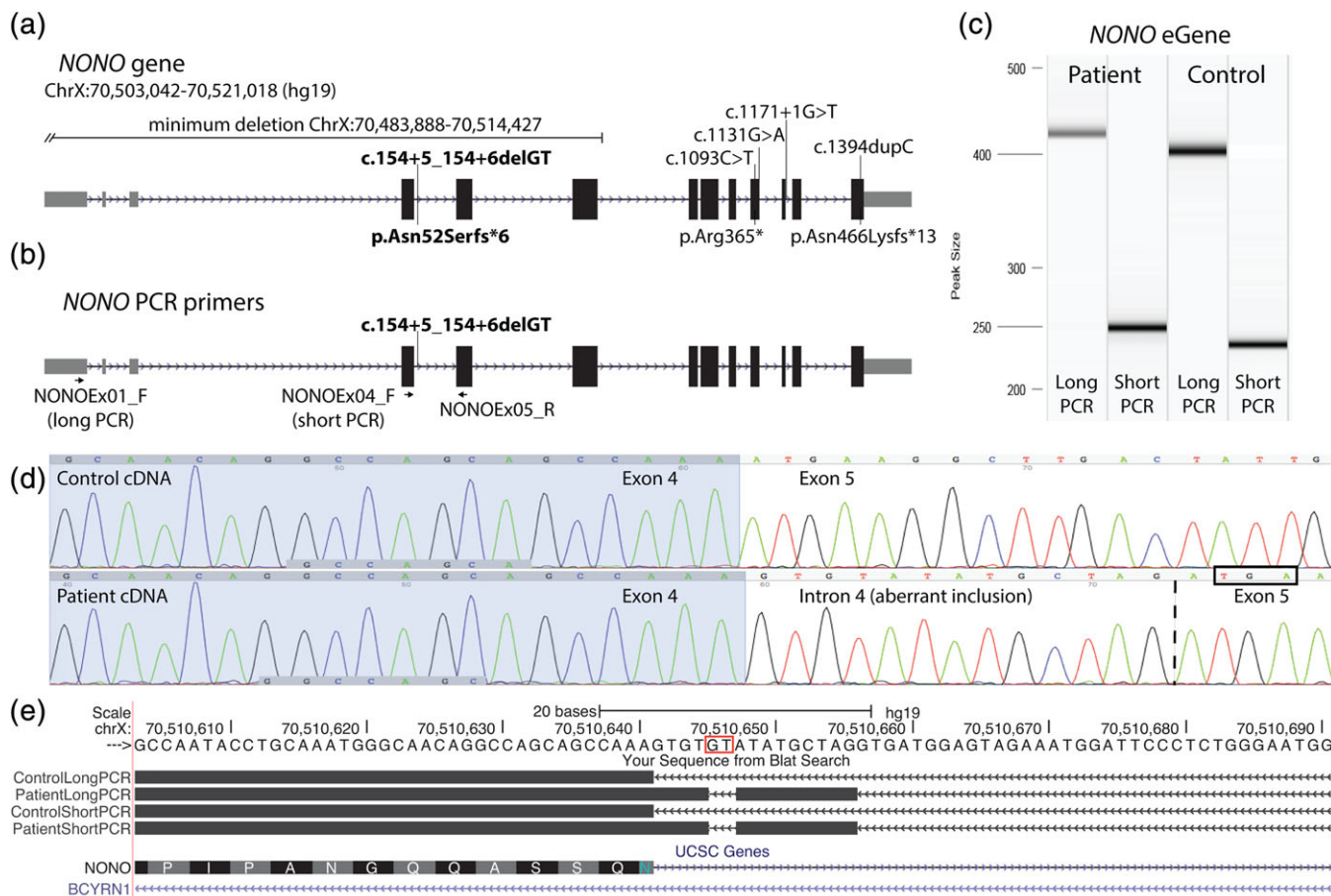


FIGURE 2 Pathogenic *NONO* variants. (a) Published pathogenic *NONO* variants, including a multi-exon deletion extending beyond the *NONO* 5'UTR. Below the gene diagram are the predicted amino acid alterations, which are unknown for the deletion and two other splicing variants. Our patient's variant is in bold. (b) Exonic *NONO* PCR primers used to amplify cDNA. A long PCR used a forward primer in the noncoding exon 1 of *NONO* while a short PCR used a forward primer in exon 4 of *NONO* (first coding exon). Both reactions used the same reverse primer in exon 5. (c) PCR products from patient and control samples visualized on an eGene. PCR products are larger in the patient than in the control. (d) Chromatograms of cDNA sequence from the patient and a control sample. The patient sample includes 13 bases of intron 4 read-through before start of exon 5 (indicated by dotted line). This frameshift introduces a premature opal stop codon (boxed). (e) *NONO* exon 4 donor site (the *NONO* gene resides within an intron of the *BCYRN1* gene). The *NONO* c.154+5_154+6delGT variant (boxed) induces the frameshift p.Asn52Serfs*6 [Color figure can be viewed at wileyonlinelibrary.com]

patient and control samples. PCR products were resolved on an eGene (Qiagen, Hilden, Germany) and a 4% agarose gel. Sanger sequencing was performed on the PCR products as described above. Primer sequences are available upon request.

3.3 | Competing interests and ethics

The authors declare no conflict of interests. This case report did not meet the definition of human subject research; thus, review and approval by institutional review board (IRB) was not required but the tenants of the Declaration of Helsinki were followed. Written informed consent for photo publication was obtained from the patient's legal guardian.

4 | RESULTS

Exome sequencing identified a maternally-inherited hemizygous 2-base pair deletion, c.154+5_154+6delGT, in intron 4 of the *NONO* gene

(NM_001145408.1), confirmed by Sanger sequencing. The *NONO* variant was not detected in maternal grandparents, indicating that it occurred as a de novo variant in the boy's mother. Figure 2a shows the variant, absent from population databases, in the context of previously described pathogenic *NONO* alterations. These include a partial gene deletion and nonsense, frameshift, and splicing variants (Mircsof et al., 2015; Reinstein et al., 2016; Scott et al., 2017).

The *NONO* c.154+5_154+6delGT variant alters a highly conserved +5 site and splicing prediction programs suggest that this deletion weakens the nearby donor and strengthens a downstream alternative donor (Desmet et al., 2009; Eng et al., 2004; Pertea et al., 2001; Reese et al., 1997; Shapiro and Senapathy, 1987). cDNA was generated from a fresh patient blood sample and PCR amplified using two sets of primers (long and short) flanking intron 4 in order to identify aberrant *NONO* transcripts (Figure 2b). In both reactions, a slightly longer PCR product was visible in the patient sample compared to an unrelated control (Figure 2c). Sanger sequencing of PCR products confirmed the use of the cryptic donor 10 bases

downstream from the intronic deletion. This creates an aberrantly spliced transcript that introduces a premature stop codon in exon 5 (of 13) of *NONO*. Translation of the transcript would produce the truncated protein (p.Asn52Serfs*6); however, the premature stop codon likely targets the transcript for nonsense-mediated decay as *NONO* protein was not detectable via immunoblot in fibroblasts from patients with splicing/frameshift *NONO* variants downstream of the c.154+5_154+6delGT variant (Mircsof et al., 2015).

To investigate potential genetic susceptibility to fungal esophagitis, all rare (<1% allele frequency) variants in immunodeficiency-related genes were interrogated during exome analysis. No plausible genetic candidates were identified.

We also examined rare variants in cardiomyopathy-associated genes to determine whether there might be additional genetic contributors to LVNC and Ebstein anomaly in this boy, and identified three inherited heterozygous variants. A maternally-inherited, missense variant was identified in *ALPK3* (rs36002219; chr15:g.85411581C>T), which has greater than a 1% allele frequency in Finns and is homozygous in four individuals in the Genome Aggregation Database (gnomAD; Lek et al., 2016). This variant is predicted by PolyPhen2 (Adzhubei et al., 2010, 2013) and PROVEAN (Choi and Chan, 2015) to be benign/neutral, and has a single likely benign classification in ClinVar (Landrum et al., 2016). A paternally-inherited, noncoding variant was detected adjacent to the 5'UTR of *HRAS* (chr11:g.534376C>T). The variant is absent from gnomAD and occurs at a highly conserved site that could affect splicing of the UTR and affect expression; however, Costello syndrome and congenital heart defects are associated with gain-of-function *HRAS* variants, whereas *HRAS* loss-of-function variants are present in the general population and predicted to be tolerated (pLI = 0.01) in the Exome Aggregation Consortium (ExAC) browser (Lek et al., 2016). Finally, a maternally-inherited, missense variant in *TTN* (rs786205395; chr2:g.179527746T>A) has six heterozygotes in gnomAD and affects a highly conserved base. It is predicted to be benign by PolyPhen2 and deleterious by PROVEAN, and is listed twice as a variant of uncertain significance in ClinVar.

5 | DISCUSSION

This report describes a two-year-old boy with developmental delays and congenital heart disease who was found to have a splicing variant in the *NONO* gene. This case adds to the spectrum of *NONO*-related disease and supports the association with Ebstein anomaly.

This novel intronic deletion in the *NONO* gene (c.154+5_154+6delGT) causes intron 4 read-through and introduces a frameshift (p.Asn52Serfs*6), which is consistent with the mechanism of previously observed pathogenic *NONO* variants (Figure 2). Although only eight cases of *NONO*-associated disease have been reported, there is substantial clinical correlation between patients with putative loss-of-function *NONO* variants (Supporting Information Table S1). Global developmental delay, nonfamilial features, and relative macrocephaly are consistent findings. Notably, abnormalities of the corpus callosum, in particular a thickened appearance, were observed in nearly all (7/8) reported patients. MRIs performed before 3 months of age in three patients were initially interpreted as normal, although two of these

patients later had MRIs interpreted as abnormal, suggesting MRI findings may become more evident over time.

Novel findings in this patient may help clinicians recognize the less frequent manifestations of *NONO*-associated disease. This child's Chiari I malformation could be a factor in his central apnea, whereas his obstructive apnea could be related to hypotonia and bulbar dysfunction. It is unclear if the single episode of fungal esophagitis was related to the *NONO* finding. Although many of the reported patients with *NONO*-associated disease had growth failure, this child is the first with documented growth hormone deficiency. Hypopituitarism could contribute to growth hormone deficiency, intermittently abnormal thyroid studies, and cryptorchidism. Furthermore, although most reported males with *NONO*-associated disease (including our patient) are pre-pubescent (Supporting Information Table S1), delayed puberty has been observed in two previous patients (Mircsof et al., 2015), implicating the hypothalamic–pituitary–gonadal axis.

Some clinical findings may be more specific but also more variable, such as LVNC cardiomyopathy in five out of eight *NONO* cases (Supporting Information Table S1). It is possible the three patients reported by Mircsof et al. never had echocardiograms and may have clinically silent LVNC, in which case this may be a fully penetrant phenotype. Of additional interest is the prior report by Scott et al. of Ebstein anomaly in a maternal half-brother of a patient with LVNC and a maternally-inherited partial deletion of *NONO*. This half-brother died at 4 days of age and could have also inherited the *NONO* partial deletion. In this context, our patient confirms the association between loss of *NONO* and Ebstein anomaly. Pathogenic variants in a single gene have previously been shown to cause both LVNC and Ebstein anomaly (Postma et al., 2011). The maternal-half sister in the previously reported family also had a heart murmur, which led us to recommend that the mother and sister in our family undergo echocardiograms. The mother's echocardiogram was normal as were cardiology exam and EKG in the sister. The sister's echocardiogram is being deferred until she is older and will not require sedation, unless she develops symptoms.

It is unknown whether the variable presentation of LVNC is inherent to *NONO* itself or relates to interactions with genetic modifiers. Recently, heterozygous variants in *GATA4* and *PTEN* were proposed as a digenic cause of LVNC cardiomyopathy (Tang et al., 2018). Both previous reports of *NONO* cases with LVNC also examined cardiomyopathy-related genes via exome analysis or multi-gene panel and identified several variants that could potentially affect the severity or type of cardiac abnormalities in patients (Reinstein et al., 2016; Scott et al., 2017).

A rare missense variant in *TTN* was detected in our patient, but its clinical significance is difficult to assess. Functional studies of another *TTN* missense variant found in a three-generation family with autosomal dominant LVNC cardiomyopathy suggested that it caused domain destabilization and impaired titin binding to telethonin (Hastings et al., 2016). *TTN* variants are reported to be extremely common in patients with noncompaction cardiomyopathy (71%) and those with multiple cardiomyopathy variants including *TTN* variants are at the highest risk of developing left ventricular systolic dysfunction (van Waning et al., 2018). It is interesting that LVNC was not reported in the first three patients with *NONO*-related disease (also among the oldest patients), but has been observed in five subsequent patients, some of whom also have additional cardiac findings. Future work will hopefully

elucidate whether loss of NONO predisposes to LVNC with variable penetrance/severity or whether it causes this phenotype in combination with co-occurring cardiomyopathy risk alleles.

ACKNOWLEDGMENTS

The authors are grateful to the family for their willingness to share this report with the medical community. The authors would also like to thank the clinical genetics and genomics scientists at ARUP laboratories and those involved with supporting the Penelope Rare and Undiagnosed Disease Program at the University of Utah.

ORCID

Colleen M. Carlston  <https://orcid.org/0000-0003-2901-8610>

REFERENCES

- Adzhubei, I., Jordan, D. M., & Sunyaev, S. R. (2013). Predicting functional effect of human missense mutations using PolyPhen-2. *Current Protocols in Human Genetics*, 76, 7.20.1–7.20.41.
- Adzhubei, I. A., Schmidt, S., Peshkin, L., Ramensky, V. E., Gerasimova, A., Bork, P., ... Sunyaev, S. R. (2010). A method and server for predicting damaging missense mutations. *Nature Methods*, 7, 248–249.
- Choi, Y., & Chan, A. P. (2015). PROVEAN web server: A tool to predict the functional effect of amino acid substitutions and indels. *Bioinformatics*, 31, 2745–2747.
- Desmet, F.-O., Hamroun, D., Lalande, M., Collod-Bérout, G., Claustres, M., & Bérout, C. (2009). Human splicing finder: An online bioinformatics tool to predict splicing signals. *Nucleic Acids Research*, 37, e67.
- Eng, L., Coutinho, G., Nahas, S., Yeo, G., Tanouye, R., Babaei, M., ... Gatti, R. A. (2004). Nonclassical splicing mutations in the coding and noncoding regions of the ATM gene: Maximum entropy estimates of splice junction strengths. *Human Mutation*, 23, 67–76.
- Hastings, R., de Villiers, C. P., Hooper, C., Ormondroyd, L., Pagnamenta, A., Lise, S., ... Gehmlich, K. (2016). Combination of whole genome sequencing, linkage, and functional studies implicates a missense mutation in Titin as a cause of autosomal dominant cardiomyopathy with features of left ventricular noncompaction. *Circulation: Cardiovascular Genetics*, 9, 426–435.
- Landrum, M. J., Lee, J. M., Benson, M., Brown, G., Chao, C., Chitipiralla, S., ... Maglott, D. R. (2016). ClinVar: Public archive of interpretations of clinically relevant variants. *Nucleic Acids Research*, 44, D862–D868.
- Lek, M., Karczewski, K. J., Minikel, E. V., Samocha, K. E., Banks, E., Fennell, T., ... Exome Aggregation Consortium. (2016). Analysis of protein-coding genetic variation in 60,706 humans. *Nature*, 536, 285–291.
- Mircsof, D., Langouët, M., Rio, M., Moutton, S., Siquier-Pernet, K., Bole-Feysot, C., ... Colleaux, L. (2015). Mutations in NONO lead to syndromic intellectual disability and inhibitory synaptic defects. *Nature Neuroscience*, 18, 1731–1736.
- Pertea, M., Lin, X., & Salzberg, S. L. (2001). GeneSplicer: A new computational method for splice site prediction. *Nucleic Acids Research*, 29, 1185–1190.
- Postma, A. V., van Engelen, K., van de Meerakker, J., Rahman, T., Probst, S., Baars, M. J. H., ... Klaassen, S. (2011). Mutations in the sarcomere gene MYH7 in Ebstein anomaly. *Circulation: Cardiovascular Genetics*, 4, 43–50.
- Reese, M. G., Eeckman, F. H., Kulp, D., & Haussler, D. (1997). Improved splice site detection in genie. *Journal of Computational Biology*, 4, 311–323.
- Reinstein, E., Tzur, S., Cohen, R., Bormans, C., & Behar, D. M. (2016). Intellectual disability and non-compaction cardiomyopathy with a de novo NONO mutation identified by exome sequencing. *European Journal of Human Genetics*, 24, 1635–1638.
- Scott, D. A., Hernandez-Garcia, A., Azamian, M. S., Jordan, V. K., Kim, B. J., Starkovich, M., ... Xia, F. (2017). Congenital heart defects and left ventricular non-compaction in males with loss-of-function variants in NONO. *Journal of Medical Genetics*, 54, 47–53.
- Shapiro, M. B., & Senapathy, P. (1987). RNA splice junctions of different classes of eukaryotes: Sequence statistics and functional implications in gene expression. *Nucleic Acids Research*, 15, 7155–7174.
- Shav-Tal, Y., & Zipori, D. (2002). PSF and p54(nrb)/NonO—multi-functional nuclear proteins. *FEBS Letters*, 531, 109–114.
- Tang, V. T., Arscott, P., Helms, A. S., & Day, S. M. (2018). Whole-exome sequencing reveals GATA4 and PTEN mutations as a potential Digenic cause of left ventricular noncompaction. *Circulation: Genomic and Precision Medicine*, 11, e001966.
- van Waning, J. I., Caliskan, K., Hoedemaekers, Y. M., van Spaendonck-Zwarts, K. Y., Baas, A. F., Boekholdt, S. M., ... Majoor-Krakauer, D. (2018). Genetics, clinical features, and long-term outcome of noncompaction cardiomyopathy. *Journal of the American College of Cardiology*, 71, 711–722.

SUPPORTING INFORMATION

Additional supporting information may be found online in the Supporting Information section at the end of this article.

How to cite this article: Carlston CM, Bleyl SB, Andrews A, et al. Expanding the genetic and clinical spectrum of the NONO-associated X-linked intellectual disability syndrome. *Am J Med Genet Part A*. 2019;1–5. <https://doi.org/10.1002/ajmg.a.61091>